Influence of curvature radius, elastic modulus, and contact velocity on real contact formation between rubber hemisphere and glass plate during contact process under a water-lubricated condition

Toshiaki Nishi

Institute of Sport Science, ASICS Corporation, 6-2-1, Takatsukadai, Nishi-ku, Kobe, Hyogo, 651-2271, Japan

ARTICLE INFO

ABSTRACT

Especially for performance in wet conditions, design of real contact formation is important to improve grip properties of footwear outer-soles and vehicle tires. Lubricant intervention between rubber and a surface is expected to be changed by the contact velocity and physical properties of the rubber: radius of curvature and elastic modulus. The influences of these parameters on real contact formation between a rubber hemisphere and glass plate in a contact process under a water-lubricated condition were investigated. The ratio between real and apparent contact areas increased with contact time as determined by these parameters. The explanation is based on dewetting behavior.

1. Introduction

Soft material tribology is an interesting field, not only industrially, but also within academic circles. In particular, rubber is an important material for improving grip and sealing properties. These properties proceed from real contact. To explain such a rubber friction behavior, many scientific contributions have been dedicated to develop theories; e.g. a Schallamach wave [1–5]. There are many contact theories which explain real contact deformation especially in the case of an unlubricated condition, as represented by the Hertz contact theory, the Johnson-Kendall-Roberts (JKR) theory [6] and the Greenwood–Williamson model [7]. It has been reported that friction force is proportional to the total real contact area A_r [8]; however, A_r can be decreased due to lubricant intervention, which leads to deterioration of grip and sealing properties. It is therefore important to control A_r, regardless of lubricant intervention. In practical applications, such as in footwear and vehicle tires, A_r is controlled by material and structural designs.

In terms of material design, it is possible to eliminate lubricant between the rubber and floor based on dewetting behavior, as explained based on wettability [9–19]. In a contact process, it has been reported that A_r increases with dewetting velocity, which is calculated from surface free energy and lubricant viscosity [9–14,19]. Additionally, in a sliding process, A_r and the friction coefficient μ increase with dewetting velocity [15–18]. Therefore, it is expected that A_r is controlled by changing the surface free energy of the rubber.

In contrast, in structural design, it is common to design tread patterns of footwear and vehicle tires. The tread groove depth and width [20–23], the tread groove orientation [22–24], the number of groove [25], and the surface roughness of groove [25,26] are helpful to increase μ. According to the Hertz contact theory, the real contact area between rubber and a surface is affected by the radius of curvature R and elastic modulus E. It has also been reported that A_r and μ are sensitive to the three-side ratio of a rubber cuboid [27]. Lubricant intervention between the tread and the floor was not considered in the above studies. Experimentally, it has been found that tread edge structure is important to break the lubricant film to make real contact between rubber and a surface. Breaking the lubricant film corresponds to real contact formation in a lubricated condition, which is related to dewetting behavior. A relationship between real contact formation, dewetting behavior, and rubber edge structure (R and E) has, however, not been clarified. In addition, a previous study suggests that dewetting behavior can be changed by changing the contact velocity, v_c, between the rubber and a surface during the contact process [19].

The purpose in this paper was to determine the relationship between rubber edge structure, v_c, and real contact formation between a rubber hemisphere and glass prism under a water-lubricated condition during the process of contact. Time dependencies of the real contact distribution and film thickness between the rubber and glass were experimentally measured. To consider the dewetting behavior, the influences of R, E, and v_c on A_r and on the real contact area for a single contact, a_r, were investigated. In this study, A_r was defined as sum of a_r.

E-mail address: toshiaki.nishi@asics.com.

Table 1
Shape and physical properties of rubber.

Rubber		(i)	(ii)	(iii)	(iv)	(v)
Curvature radius, mm		7.62	5.08	10.30	7.60	7.62
Elastic modulus, MPa		2.30	2.30	2.30	1.26	3.53
Arithmetical mean height S_a, μm		0.18	0.16	0.17	0.18	0.16
Surface free energy, mJ/m^2	Dispersion	11.0	11.0	11.0	10.6	10.6
	Polar	1.7	1.7	1.7	1.8	1.8
	Total	12.7	12.7	12.7	12.4	12.4

2. Experimental methods

2.1. Sample preparation

In order to investigate the influences of R and E on real contact formation, hemispheres of silicon rubber (Sylgard 184, Dow Corning Toray Co., Ltd., Japan) with different R and E were prepared, as shown Table 1. Titanium oxide (A150, Sakai Chemical Industry Co., Ltd., Japan) was added to the silicon at 10 vol% to ensure that light was reflected in a total reflection method, as explained in a previous study [28]. Three types of concave lens (TS-0250S, Sugitoh Co., Ltd., Japan, S-SLB-10-15N, SIGMAKOKI Co., Ltd., Japan, and SLB-10-20N, SIGMA-KOKI Co., Ltd., Japan) were used to mold the rubber to control R. E was changed by changing the ratio of cross-linking agent (5.0, 10.0, and 20.0 mass%) to silicon rubber. Table 1 shows that there was no difference in surface roughness and surface free energy between the rubbers tested. E was quantified by a dynamic viscoelastic measurement device (Reogel E4000, UBM Co., Ltd., Japan). To measure R and surface roughness, a One-Shot 3D measuring macroscope (VR3000, Keyence Corporation, Japan) was used. As the index of surface roughness, arithmetical mean height S_a was calculated from the 0.100 mm-square geometry of the undermost rubber surface where real contact would be formed. The effect of R on S_a was eliminated by plane correction of the measured geometry by using the accompanying software (VR-H1A, Keyence Corporation, Japan). To calculate surface free energy based on the Kaelble and Uy theory [29], the contact angles of ion-exchanged water and diiodomethane (Wako 1st grade, Wako Pure Chemical Industries, Ltd.) with a contact angle meter (DMs-401, Kyowa Interface Science Co., Ltd., Japan).

2.2. Experimental apparatus

To discuss influences of R, E, and v_c on A_r and a_r, distributions of real contact and film thickness between the rubber hemispheres and glass prism (084.4L100-45DEG-6P-4SH3.5, SIGMAKOKI Co., Ltd., Japan) were quantified for values of v_c from 0.10 to 1.00 mm/s in increments of 0.1 mm/s, and based on a total reflection method and light interferometry by using the original experimental apparatus as shown

in the Fig. 1 [19,28]. The load cell (TL201Ts, Trinity-Lab Inc., Japan) and the electric cylinder (EACM4D30AZAC, Oriental Motor Co., Ltd., Japan) are already mounted to investigate relationship between friction and dewetting behaviors in the future. Ion-exchanged water was used as the lubricant. And the water depth was set at about 2.5 mm. The normal force increased to 0.0981 N, as the rubber got close to the grass. The pixel format, pixel size, and frame rate of a charge-coupled device (CCD) camera (AT-030MCL, JAI Ltd., Japan) were set at 12 bit, $3.6 \times 3.6 \, \mu m^2$, and 100 fps, respectively. The tests were conducted at 23.8–25.0 °C and 71–75 %RH.

3. Results

3.1. Time dependency of contact condition between rubber and glass

The time dependencies of real contact distribution and film thickness for the case of rubber (i) at $v_c = 0.50$ mm/s is shown in Fig. 2. Real contact and film thickness are indicated by red and blue, respectively. Real contact and film thickness are quantified based on the previous study [28]. The onset time of real contact was defined as $t = 0.00$ s. As explained in the previous study, the contact process was completed at $t = 0.08$ s in this case [19]. Fig. 2 also indicates that the number of real contacts N and the size of each real contact increased. The film thickness around the real contacts increased, which explained by dewetting of the lubricant from the real contact to the outside of the contact [13]. Fig. 3 shows the time dependencies of A_r and N and the relationship between N and A_r for the same case in Fig. 2. A_r was defined as total real contact area between the rubber and the glass. N was defined as the number of completely separate real contacts whose area is large than 1 pixel by using MATLAB software (R2016b, The MathWorks, Inc., USA). At $t = 0.01$–0.08 s, A_r and N increased, and the rate of increase of A_r decreased at $t = 0.08$ s when the contact process was completed. These results suggest that A_r and N increased with apparent contact area A, as calculated by the Hertz contact theory, at $t = 0.01$–0.08. In particular, the observation that N increased linearly at $t = 0.01$–0.08 s indicated that N is proportional to A, given a proportional relation between A and t. In contrast, A_r continued increasing by lubricant localization at $t = 0.08$–10.00 s while the rubber remained stationary. In addition, N decreased gradually at $t = 0.08$–10.00 s, which is explained by coalescence between real contacts. These results explains that N increased with A_r at $A_r < 0.1 \, mm^2$ and that this increasing rate got degreased at $A_r > 0.1 \, mm^2$, as shown in Fig. 3(c).

3.2. Influence of radius of curvature, elastic modulus, and contact velocity

Fig. 4 shows the influences of R, E, and v_c on A_{r0}, which is defined as A_r at $t = t_0$. t_0 is defined as the time when $v_c t$ is equal to the approach distance δ calculated in the Hertz contact theory, in other word, the
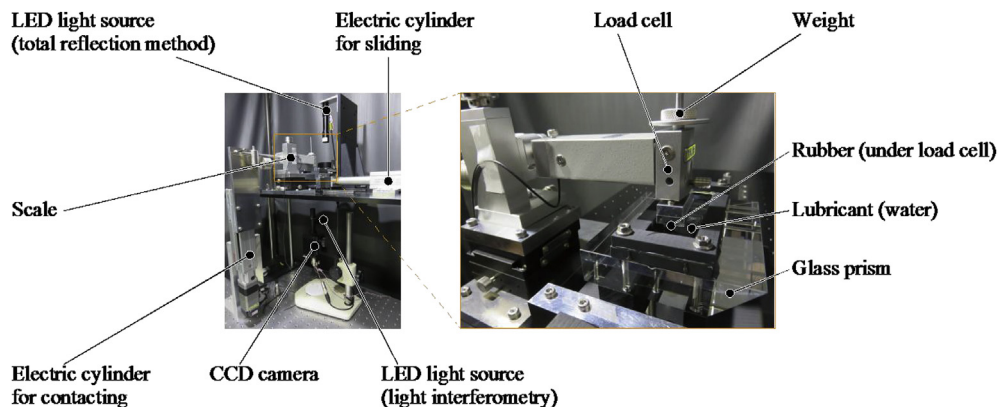
Fig. 1. Experimental apparatus picture.